HEAT TRANSFER IN NATURAL CONVECTION FROM HORIZONTAL HEAT-TRANSFER SURFACES FACING DOWNWARD

P. M. Brdlik and I. A. Turchin

Inzhenerno-Fizicheskii Zhurnal, Vol. 14, No. 3, pp. 470–477, 1968

UDC 536.25

Approximate solutions are presented for the transfer of heat in two regions, i.e., a region in which the inertial and viscous forces are of identical order of magnitude, and the region of creep flow. The experiments carried out with air over a wide range of Ra_x numbers yield results in good agreement with the solutions.

The initial experiments—by Wise [1]—into the distribution of local heat-transfer coefficients under conditions of natural convection from a downturned horizontal heat-transfer surface disclosed two characteristic regions of change in the heat-transfer coefficient. Near the edges of the plate it was found that the heat-transfer coefficient increased sharply, according to the law $Nu_x \sim Gr_x^{1/5}$. At the center of the plate the heat-transfer coefficient remains virtually constant independent of the longitudinal coordinate x, i.e., $Nu_x \sim Gr_x^{1/3}$.

The interferometric patterns of the temperature fields (Fig. 1) which we obtained for the boundary layer serve also to confirm this type of change in the heat-transfer coefficients. For a small plate 5 cm in width (the top picture in Fig. 1), the thickness of the boundary layer increases continuously from the edges to the center of the plate, while the heat-transfer coefficient diminishes according to the law $Nu_x \sim Gr_x^{1/5}$. For a large plate 20 cm in width (the bottom picture in Fig. 1) we now find two characteristic zones of variation in the thickness of the boundary layer and in the heat-transfer coefficient: virtual constancy at the center of the plate, and reduction toward the edges of the plate.

Proceeding from this physical representation, we can divide the boundary layer of a horizontal plate—whose heated surface is facing downward—into two flow regions. The region around the plate edges is characterized by an approximately identical order of inertial and viscous forces; the region in the center of the plate is characterized by creep flow in which viscosity forces predominate.

For the first region, where we find a pronounced change in the heat-transfer coefficient from the longitudinal coordinate, the hydrodynamics and heat transfer can be described by the following system of boundary-layer equations [2]:

$$u\frac{\partial u}{\partial x}+v\frac{\partial u}{\partial y}=-\frac{\partial P}{\partial x}+\nu\frac{\partial^2 u}{\partial y^2}, \tag{1}$$

$$\frac{\partial P}{\partial y}=g\beta\theta, \tag{2}$$

$$\frac{\partial u}{\partial x}+\frac{\partial v}{\partial y}=0, \tag{3}$$

$$u\frac{\partial\theta}{\partial x}+v\frac{\partial\theta}{\partial y}=a\frac{\partial^2\theta}{\partial y^2} \tag{4}$$

(see Fig. 1 for the location of the coordinate). In view of the symmetry of flow, the coordinate x varies in limits from 0 to $l/2$.

The integral relationship for system (1)–(4) have the form

$$\frac{\partial}{\partial x}\int_0^\delta u^2dy=-\nu\left.\frac{\partial u}{\partial y}\right|_{y=0}-\frac{\partial}{\partial x}\int_0^\delta Pdy, \tag{5}$$

$$\int_y^\delta\frac{\partial P}{\partial y}dy=g\beta\int_y^\delta\theta\,dy, \tag{6}$$

$$\frac{\partial}{\partial x}\int_0^{\delta_t}u\theta\,dy=-a\left.\frac{\partial\theta}{\partial y}\right|_{y=0}. \tag{7}$$

The approximate solution to the problem was sought by resorting to the Karman-Pohlhausen method for

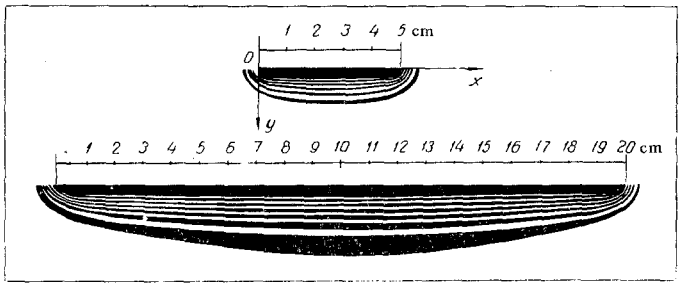

Fig. 1. Interference temperature-field pictures near horizontal surfaces, with their heated sides downward, with natural convection in an infinite air volume.

the following boundary conditions:

$$y = 0 \left| \begin{array}{l} u = v = 0,\ \theta_w = t_w - t_\infty = \text{const}, \\ \dfrac{\partial^2 \theta}{\partial y^2} = 0, \end{array} \right. \quad (8)$$

$$y = \delta \left| \begin{array}{l} u = 0,\ \dfrac{\partial u}{\partial y} = 0,\ \theta = 0, \\ \dfrac{\partial \theta}{\partial y} = 0,\ P = 0. \end{array} \right. \quad (9)$$

The distribution of temperatures and velocities within the boundary layer is written in polynomial form:

$$\theta = \theta_w \left(1 - \frac{3}{2}\frac{y}{\delta_t} + \frac{1}{2}\frac{y^3}{\delta_t^3}\right), \quad (10)$$

$$u = -u_1 \frac{y}{\delta}\left(1 - \frac{y}{\delta}\right)^2, \quad (11)$$

which satisfy boundary conditions (8) and (9). Here u_1 is an unknown expressed in units of velocity.

Equations (5)–(7) are integrated in the assumption that the thicknesses of the hydrodynamic and thermal boundary layers are equal. This assumption is not too gross for natural convection. In any event, the comparison (Fig. 2) which we carried out between the exact solutions obtained by Ostrach [3], Sparrow, and Gregg [4] for a laminar boundary layer in natural convection on vertical surfaces for Pr = 10^{-3}–10^3 and the approximate solution obtained in [5] in the assumption that the boundary layers were equal resulted in a maximum divergence of boundary-layer discharge characteristics (α_x and τ_w) that did not exceed ±3%.

Substitution of profiles (10) and (11) into system (5)–(7), with consideration of boundary conditions (8) and (9), yields

$$\frac{\delta}{x} = 3.33\,(\mathrm{Gr}_x\,\mathrm{Pr})^{-1/5}\,(2 + \mathrm{Pr}^{-1})^{1/5}, \quad (12)$$

$$u_1 = 5.9\,\frac{a}{x}\,(\mathrm{Gr}_x\,\mathrm{Pr})^{2/5}\,(2 + \mathrm{Pr}^{-1})^{-2/5}. \quad (13)$$

The local heat flow at the wall is found from (10):

$$q_w = \frac{3}{2}\,\lambda\,\frac{\theta_w}{\delta} =$$

$$= 0.45\,\lambda\,\frac{\theta_w}{x}\,(\mathrm{Gr}_x\,\mathrm{Pr})^{1/5}\,(2 + \mathrm{Pr}^{-1})^{-1/5} \quad (14)$$

and the local Nusselt number

$$\mathrm{Nu}_x = 0.45\,(\mathrm{Gr}_x\,\mathrm{Pr})^{1/5}\,(2 + \mathrm{Pr}^{-1})^{-1/5}. \quad (15)$$

For air (Pr = 0.72)

$$\mathrm{Nu}_x = 0.351\,(\mathrm{Gr}_x\,\mathrm{Pr})^{1/5} = 0.329\,\mathrm{Gr}_x^{1/5}. \quad (16)$$

The average Nusselt number for a plate completely within the first flow region is

$$\overline{\mathrm{Nu}} = \frac{\bar{\alpha} l}{\lambda} = 0.99\,(\mathrm{Gr}_l\,\mathrm{Pr})^{1/5}\,(2 + \mathrm{Pr}^{-1})^{-1/5}. \quad (17)$$

For air (Pr = 0.72) we have

$$\overline{\mathrm{Nu}} = 0.776\,(\mathrm{Gr}_l\,\mathrm{Pr})^{1/5}, \quad (18)$$

which is smaller by 7.5% than the exact Stewartson solution [6], obtained for the average heat-transfer

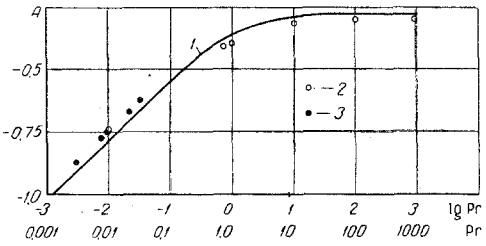

Fig. 2. Comparison of exact heat-transfer solutions with laminar natural convection on vertical surfaces with approximate solution ($A \equiv \mathrm{Nu}_x/(\mathrm{Gr}_x\mathrm{Pr})^{1/4}$): 1) Squire's approximate solution [5]; 2) Ostrach's exact solution for Pr = 0.01, 0.72, 1.0, 10, 100, and 1000; 3) exact solution of Sparrow and Gregg [4] for liquid metals with Pr = 0.03, 0.02, 0.01, 0.008, and 0.003.

coefficient when Pr = 0.72:

$$\overline{\mathrm{Nu}} = 0.841\,(\mathrm{Gr}_l\,\mathrm{Pr})^{1/5}. \quad (19)$$

The Fishenden and Saunders experiment [7] on the average heat-transfer coefficient in air yield the relationship

$$\overline{\mathrm{Nu}} = 0.81\,(\mathrm{Gr}_l\,\mathrm{Pr})^{1/5}, \quad (20)$$

which is only 4% lower than our approximate solution.

Thus, for the first flow region the approximate solution yields satisfactory agreement with the exact solution and experiment.

For the second region, i.e., the region of creep flow, where the heat-transfer coefficient is virtually independent of the longitudinal coordinate, the equations for the creeping "boundary layer" in our coordinate system can be written in analogy with the equations for the forward point [8]:

$$\frac{d^2 v}{dy^2} - \frac{g\beta\theta}{\nu} = 0, \quad (21)$$

$$\frac{d^2\theta}{dy^2} = \frac{v}{a}\,\frac{d\theta}{dy}. \quad (22)$$

The concept of "boundary layer" is retained here in the sense that the effect of the heated wall is extended to a layer small in comparison with the dimensions of the plate (see Fig. 1), thus making it possible to neglect the derivatives with respect to x in Eqs. (21) and (22). Here, as in the first region, we will seek the approximate solution by resorting to the Karman-Pohlhausen method.

We assume the following velocity distribution in the "boundary layer" (within the layer in which the heated wall exerts an effect):

$$v = -v_1 \left(\frac{y}{\delta}\right)^2. \qquad (23)$$

It satisfies the wall boundary condition v = 0 when y = 0. At the outside edge of the boundary layer we have y = δ,

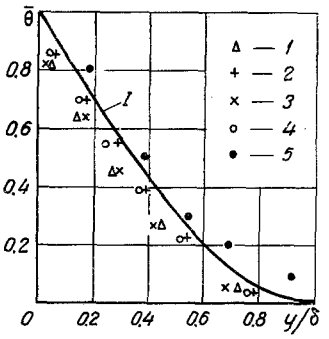

Fig. 3. Dimensionless temperature profile within the first flow region ($\bar{\theta} = \theta/\theta_w$), $y/\delta = (y/4.25x)(Gr_x Pr)^{1/5}$: 1) approximation of (10) with substituion of δ from solution (12); 1) $Ra_x = 7 \cdot 10^3$; 2) $8 \cdot 10^3$; 3) $2.4 \cdot 10^4$; 4) $2.8 \cdot 10^4$; 5) $Ra_x = 2.4 \cdot 10^3$ [1].

u = 0, du/dx = 0, and it follows from the continuity equation that $v = -v_1 = \text{const}$, which is also satisfied by distribution (23).

The temperature distribution in the "boundary layer" is expressed in the form of the polynomial

$$\theta = \theta_w \left(1 - \frac{1}{5}\frac{y}{\delta} - \frac{4}{5}\frac{y^3}{\delta^3}\right), \qquad (24)$$

which satisfies the boundary conditions

$$y = 0, \quad \theta = \theta_w, \quad \frac{\partial^2 \theta}{\partial y^2} = 0,$$

$$y = \delta, \quad \theta = 0. \qquad (25)$$

Integration of Eqs. (21) and (22) with respect to the thickness of the "boundary layer," with consideration of (23) and (24), leads to

$$\frac{\delta}{x} = 2.32\,(Gr_x\,Pr)^{-1/3}. \qquad (26)$$

With consideration of (26), from distribution (24) we find the heat flow at the wall:

$$q_w = 0.0862\,\frac{\lambda}{x}\,\theta_w\,(Gr_x\,Pr)^{1/3}. \qquad (27)$$

The local heat-transfer coefficient for the second region (the creep-flow region) is then expressed by

$$Nu_x = 0.0862\,(Gr_x\,Pr)^{1/3}. \qquad (28)$$

Equating (15) and (28), we find the value of the complex $(Gr_x Pr)_*$, separating the two flow regions:

$$(Gr_x\,Pr)_* = 2.43 \cdot 10^5\,(2 + Pr^{-1})^{-3/2} \qquad (29)$$

or for air (Pr = 0.72)

$$(Gr_x\,Pr)_* = 3.88 \cdot 10^4. \qquad (30)$$

The average Nusselt number for a plate whose heated surface is turned downward was determined experimentally in air by Novozhilov [9], who derived the following relationship for a 0.91 × 0.91 m in the region $Gr_l Pr \gg 3.88 \cdot 10^4$:

$$\overline{Nu} = 0.085\,(Gr_l\,Pr)^{1/3}, \qquad (31)$$

which differs by only 1.5% from the theoretical solution of (28). The McAdams [10] generalization of the experiments on the average heat transfer for Pr > 0.7 yields the following theoretical formula for plates whose heated sides are turned downward:

$$\overline{Nu} = 0.104\,(Gr_l\,Pr)^{1/3}, \qquad (32)$$

which exceeds the Nu value of solution (28) by 17%.

Such agreement between (28) and the generalization of the McAdams experiments on the average heat transfer can be treated as completely satisfactory, since the experimental points, on the average, yield a scatter about the approximating curve (32) of ±10%. Moreover, the increase in the heat transfer toward the edges of the plate is not accounted for by formula (28), which may result in a substantial exaggeration of the coefficient in (28) for comparatively small plates (see formulas (33)).

The average Nusselt number for a plate of length *l* for which $(Gr_x Pr) > (Gr_x Pr)^*$ is given by

$$\overline{Nu}_l = 7.13\,(2 + Pr^{-1})^{-1/2} + 0.0862\,(Gr_l\,Pr)^{1/3} \qquad (33')$$

or for air (Pr = 0.72)

$$\overline{Nu}_l = 3.88 + 0.0862\,(Gr_l\,Pr)^{1/3}. \qquad (33'')$$

In many cases it is impossible for the comparison of the theoretical solutions relative to the experiments on the average heat transfer to serve as a reliable guarantee of validity for the physical model on which the solutions are based. It is therefore of considerable interest to compare the derived approximate solutions with the experiments on local heat transfer.

In the light of the inadequate experimental data on local coefficients, we set up an experiment whose

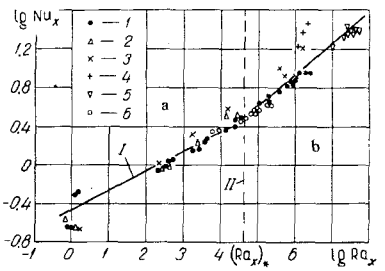

Fig. 4. Local heat transfer under conditions of natural convection in the air near horizontal plates with their heated surfaces downward. I) according to (16) for the first region and according to (28) for the second one; II) values of $(Ra_x)_*$ according to (30); 1 and 2) on the plate with *l* = 200 and 50 mm; 3) 160 mm [1]; 4) 720 mm [11]; 5) 910 mm [9]; 6) 100 and 200 mm [12] a—region on of 1/5 law; b—region of 1/3 law).

purpose was to provide the maximum range of Ra_x numbers and to establish the values of $(Ra_x)_*$ in the transition zone separating the two characteristic heat-transfer regions.

The experiment was carried out in air on two brass plates which were 50 and 200 mm wide, each exhibiting a length of 400 mm and a thickness of 5 mm. The constancy of the plate-surface temperature was ensured by an extremely tight winding of nichrome wire and the sufficient thickness of the plate. The temperature field in the boundary layer and the plate-surface temperature were measured by means of an interferometer. To achieve the required accuracy in measuring the temperature fields, we positioned the models lengthwise along the lightbeam of the interferometer. These specially adopted measures to prevent the effect of external disturbances at the boundary layer of the plate proved to be unnecessary, and it developed during the course of the experiment, since the boundary layer for a plate whose heated side is turned down was extremely resistant to external disturbances. The local heat-transfer coefficients were determined from the temperature profiles. Since the physical parameters of the air in the experiments of [1, 9, 11, 12] were taken for a wall temperature t_w, we also took t_w as the decisive temperature.

The experiments were carried out at heated temperatures ranging from 10 to 70° C, and the local Rayleigh numbers varied in the limits $Ra_x = 0.7-2.5 \cdot 10^6$.

The experimental results are shown in Figs. 3 and 4. Figure 3 shows a comparison of the dimensionless temperature profiles (obtained experimentally in the first flow region) with the profile determined from (10) on substitution into the latter of the value of δ from (17) for Pr = 0.72. Here we also find the temperature profile derived in the Weise experiments [1]. As we can see from Fig. 3, the experimental temperature profiles are in satisfactory agreement with the approximate solution.

The experimental data of the various authors [1, 9, 11, 12] on the local transfer of heat in air from a horizontal plate whose heating surface is facing downward are shown in Fig. 4. The range of generalization for the experimental data is $Ra_x = 0.7-5 \cdot 10^7$. Here we also find the following approximate solutions: (16) for the first region and (28) for the second heat-transfer region. The agreement between the approximate solutions and the experiment must be regarded as satisfactory. The slight overstatement of the experimental values of α_x relative to the solution—as given in [1] and [11]—can be explained by the strong influence of radiative heat exchange in these references.

NOTATION

x and y are the transverse and longitudinal coordinates; θ is the excess temperature; t is the temperature; l is the plate width; δ is the boundary-layer thickness; P is the excess pressure; ρ is the density; u_1 is the typical velocity; q_w is the specific heat flux on wall; u and v are the longitudinal and transverse velocities; Ra is the Rayleigh number. Symbols: x is the local value; dash denotes the mean value; w denotes the wall; ∞ denotes the undisturbed flow; l denotes the plate width; * denotes the transition value.

REFERENCES

1. R. Weise, Forschung a. d. Gebiete des Ingenieurwesens, **6**, no. 6, 1935.
2. S. Ostrach, NACA, Tech. Note, 2635, 1952.
3. S. Ostrach, NACA, TR 1111, 1953.
4. E. Sparrow and J. Gregg, NACA, TN 3508, 1955.
5. H. Squire, The State of the Art in High-Speed Aerodynamics, Vol. II [Russian translation], IL, 1956.
6. K. Stewartson, ZAMP, Brief Reports, Vol. IX-a, 1958.
7. M. Fishenden and O. Saunders, An Introduction to Heat Transfer, Oxford, 95, 1950.
8. V. P. Motulevich, Nauchnye trudy MLTI, no. 9, 1958.
9. V. I. Novozhilov, ZhTF, 1, no. 2–3, 1931.
10. McAdams, Heat Transmission, 2-nd edition, 1942.
11. V. S. Zhukovskii, ZhTF, 1, no. 2–3, 1931.
12. V. A. Smirnov, Dissertation, Moscow Technological Institute of Light Industry, Moscow, 1964.

13 May 1967

Institute of Structural Physics, Moscow